UNIVERSITÄT
LEIPZIG

Advanced Physics Laboratory
Faculty of Physics and Earth System Sciences

High-Resolution Gamma Spectrometry
with the Ge-Semiconductor Detector

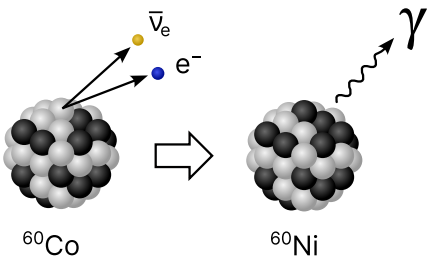

Summary

In this experiment, the gamma radiation of radioactive nuclides is investigated. For this purpose, a gamma spectrometer with a high-resolution germanium semiconductor detector is used. It is first calibrated, then the gamma spectra of various samples are recorded. The spectra are subsequently used to identify the individual radionuclides based on their known gamma energies and to deduce the respective decay chains.

David Plotzki
Leipzig, May 24, 2024

Contents

Tasks

1. Finding Optimal Settings

1.1 Use the radioactive ^{137}Cs sample to investigate the dependency of the line width (FWHM) and of the count rate ("peak height") on the rise time τ of the main amplifier at a detector operating voltage of 2500 V. For this purpose, measure spectra between $\tau = 0.5\,\mu s \ldots 12\,\mu s$. Use about every third setting step that is selectable in the software.

1.2 Determine the optimal rise time and justify your choice.

2. Calibration and Characterization

2.1 Calibrate the spectrometer at a detector operating voltage of 2500 V and the optimal rise time you have determined. Use the known gamma energies of the following radionuclides: ^{22}Na, ^{60}Co, ^{133}Ba and ^{137}Cs. The 1332 keV peak of ^{60}Co should be approximately at channel number 4000 (out of a total of 8192).

2.2 Use the 1332 keV peak of the ^{60}Co sample to determine the resolution R and the peak-to-Compton ratio of the spectrometer.

3. Investigation of Background Radiation

3.1 Record a spectrum of the background radiation with a fixed measurement time of about 30 min (or more).

3.2 Determine the energies and intensities of the occurring gamma radiation and identify the corresponding nuclides.

Use the measured spectrum in the following tasks to subtract the background radiation from the spectra of the measured samples. For this purpose, all spectra must be normalized to their respective recording time.

4. Investigation of Natural Samples

4.1 Record gamma spectra of a soil sample, a rock sample, and at least one artificial object.

4.2 Determine the energies and intensities of the emitted gamma lines as well as the corresponding nuclides and decay chains.

5. Identification of Unknown Substances

Two unknown samples are to be examined.

5.1 Record a gamma spectrum for each sample.

5.2 Determine the occurring radionuclides. Which natural decay chain can you identify?

Determine the parent nuclides by comparing the measurement results with the nuclide tables of the natural decay chains. Conclude from this the elemental composition of the sample.

Radiation Protection Guidelines

In this experiment, work is carried out with radioactive samples that emit ionizing radiation. To protect yourself and others in the vicinity, the following special behaviors must be adhered to when handling the samples.

- In general, the basic rules of radiation protection apply when handling radioactive materials:
  - Keep a distance,
  - Limit the time spent in close proximity to the radiation source,
  - Use shielding to protect yourself from radiation.
- Everyone must organize and carry out their work in such a way that other persons are not endangered.
- Defects in radiation protection equipment and/or damages to the emitters due to handling during the lab course must be reported immediately to the radiation protection officer (RPO).
- The emitters must not be touched with unprotected hands.
- Strict work discipline is required when handling radioactive material.
- The consumption of food and beverages (eating, drinking, smoking, etc.), as well as the use of cosmetics and taking medication, are prohibited during the handling of radioactive emitters.
- Touching exposed body parts (skin, face, hair, etc.) should be avoided as much as possible while working with the radioactive material.
- After experimental work with the radioactive material, hands must be washed thoroughly.
- Any manipulation of the radioactive samples that is not related to the experiment is prohibited. **The emitters must be protected from damage. No force may be applied.**
- All unused radioactive emitters must be stored securely, protected from unauthorized access and shielded in compliance with storage regulations.
- The local RPO points out according to §63(5) StrlSchV (Radiation Protection Ordinance) that a **pregnancy** must be reported as early as possible in view of the risks of exposure to the unborn child. To protect the unborn child, working with ionizing radiation is not allowed during pregnancy.

Behavior in Case of Emergency

Behavior in case of contamination of people, property, and the environment:

- **Rule 1: People have absolute priority!**
- **Rule 2: Consider further steps with care and act prudently!**

In case of contamination (e.g., due to leakage or damage of a source), the second person involved in the experiment (not contaminated) must immediately alert the local RPO; the contaminated person remains passive until the RPO arrives.

Recommended Literature and Online Materials

The following books are available for loan from the Leipzig University Library. Some are also available online (via library login or university VPN).

- **Gordon Gilmore:** ***Practical Gamma-Ray Spectrometry,*** 2nd edition (2008), Wiley

  A very good, easy-to-understand introduction to the topics of radioactivity and gamma spectrometry. This experimental guideline is primarily based on Gilmore's book.

  - ISBN: `978-0-470-86196-7`
  - Online: `https://doi.org/10.1002/9780470861981`

- **Kenneth S. Krane:** ***Introductory Nuclear Physics,*** Wiley (1987)

  A very comprehensive introduction to nuclear physics and the principles of radiation detection. For this experiment, especially the chapters from *Unit II: Nuclear Decay and Radioactivity* are of interest.

  - ISBN: `978-0-471-80553-3`

- **NuDat 3.0 Database** of the *National Nuclear Data Center* at the *Brookhaven National Laboratory* of the *US Department of Energy.*

  Interactive nuclide chart with connected nuclide database, which contains, among other things, the gamma lines of the radionuclides.

  - Online: `https://www.nndc.bnl.gov/nudat3/`

1 Nuclear Physics and Radioactivity

1.1 Basic Concepts of Nuclear Physics

Atomic nuclei consist of protons and neutrons, the so-called **nucleons**. The number of protons in the nucleus is referred to as the **atomic number** Z, and the number of neutrons as the **neutron number** N. The total number of nucleons in the nucleus is the **mass number** A:

$$A = Z + N. \tag{1}$$

A **nuclide** is fully described by its specific number of protons Z and neutrons N. To clarify which nuclide is meant, a notation has been established which displays the total nucleon number A and the number of protons Z together with the element symbol Sy:

$$^{A}_{Z}\mathrm{Sy} \quad \text{e.g. } ^{137}_{55}\mathrm{Cs} \text{ or } ^{22}_{11}\mathrm{Na}. \tag{2}$$

Since the chemical symbol and the atomic number Z provide equivalent information, the atomic number is often omitted in simplified notation: ^{137}Cs, ^{22}Na.

In chemical reactions, the electron shell plays the main role. Therefore, the numbering and naming of elements in the periodic table refers to the number of electrons in the atomic shell, and thus equally to the number of protons in the nucleus, i.e., the atomic number Z. However, atomic nuclei can also differ in the number of neutrons. Elements with the same atomic number Z but different neutron number N are referred to as **isotopes.** To indicate that an atomic nucleus is radioactive, the terms **radionuclide** or, if relevant in the respective context, **radioisotope** have been established.

1.2 Gamma Radiation

Gamma radiation is highly energetic electromagnetic radiation. It is emitted by atomic nuclei when they relax from an excited energetic state to the ground state. In the electromagnetic spectrum, gamma radiation and X-rays overlap in a certain energy range (Fig. 1). In contrast to gamma radiation, which originates in the atomic nucleus, X-rays usually refer to radiation from the acceleration, deceleration, or energy change of charged particles, especially the electrons of the atomic shell.

1.3 Radioactive Decays

Excited nuclear states that lead to the emission of gamma radiation are often the result of radioactive decays. In this process, an unstable atomic nucleus (the parent nuclide, X) transforms into a lighter nucleus (the daughter nuclide, Y) by emitting particle radiation.

$$\underset{\text{Parent nuclide}}{\mathrm{X}} \longrightarrow \underset{\text{Daughter nuclide}}{\mathrm{Y}} + \underset{\text{Particle}}{\mathrm{P}} + \underset{\text{Energy}}{Q} \tag{3}$$

A decay is only possible if the mass of the parent nuclide is greater than the sum of the masses of all resulting particles (i.e., if $Q \geq 0$):

$$m_{\mathrm{X}} \geq m_{\mathrm{Y}} + m_{\mathrm{P}}. \tag{4}$$

The total energy released a in radioactive decay is referred to as the Q-value. This results from the

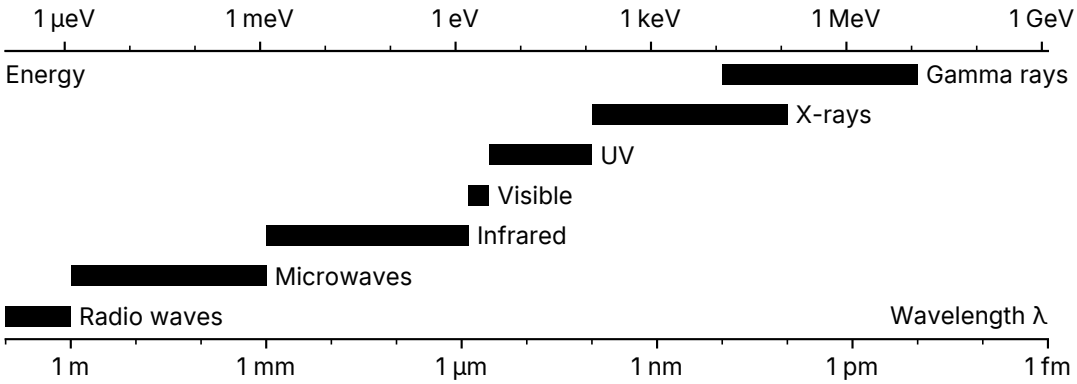

Figure 1: The electromagnetic spectrum.

mass difference between the parent atom (in its neutral ground state) and the decay products (for daughter nuclides also in their neutral ground states):

$$Q = \Delta m \cdot c^2 = (m_X - m_Y - m_P) \cdot c^2. \quad (5)$$

The Q-value thus contains the kinetic energies of the decay products: in the case of the daughter nuclide Y, this is referred to as the *recoil energy*. Additionally, the Q-value contains, if applicable, the excitation energy of the daughter nucleus, which relaxes to its ground state by emitting gamma radiation.

The characteristic gamma emission energies as a result of a radioactive decay are conventionally attributed to the parent nuclide, even though they are emitted by the daughter nuclide.

1.4 Decay Law

Considering an ensemble of N unstable, radioactive nuclei, the decay rate $\mathrm{d}N/\mathrm{d}t$ is proportional to the number of nuclei:

$$A = -\frac{\mathrm{d}N}{\mathrm{d}t} = \lambda N. \quad (6)$$

Here, A is the current **activity** of the sample. It is given in Becquerel ($1\,\mathrm{Bq} = 1/\mathrm{s}$). The **decay constant** λ determines how often a decay occurs in the ensemble. Solving equation (6), we obtain the **decay law:**

$$N(t) = N_0 \mathrm{e}^{-\lambda t}. \quad (7)$$

This allows us to calculate how many nuclei will likely still be present at time t, given an initial population N_0 at time $t_0 = 0$. The **mean lifetime** τ of a nucleus is then

$$\tau = \frac{1}{\lambda}, \quad (8)$$

while the **half-life** $t_{1/2}$ is defined as the time in which half of the nuclei will likely have decayed:

$$t_{1/2} = \frac{\ln 2}{\lambda}. \quad (9)$$

1.5 α Decay

During alpha decay, helium nuclei (alpha particles) are emitted, resulting in the nucleus losing two protons and two neutrons.

$$^{A}_{Z}\mathrm{X} \longrightarrow {}^{A-4}_{Z-2}\mathrm{Y} + {}^{4}_{2}\mathrm{He}^{2+} + Q \quad (10)$$

This type of decay typically occurs in heavier atomic nuclei ($Z > 83$). An example is the alpha decay of Americium-241:

$$^{241}_{95}\mathrm{Am} \longrightarrow {}^{237}_{93}\mathrm{Np} + {}^{4}_{2}\mathrm{He}^{2+} + 5.638\,\mathrm{MeV}. \quad (11)$$

The decay energy Q is divided according to the conservation of momentum between the alpha particle and the daughter nuclide. This results in a defined kinetic energy for the alpha particles from such a decay, which allows for alpha particle spectrometry in addition to gamma spectrometry.

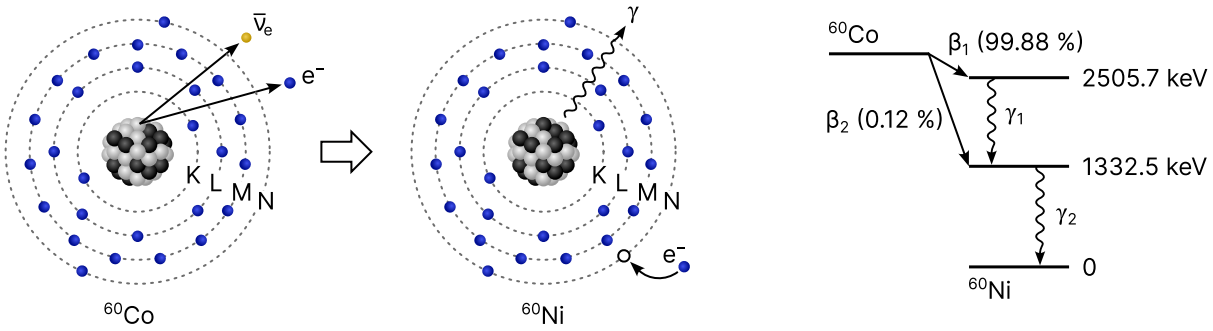

Figure 2: The β^- decay of Cobalt-60: graphical representation and energy level diagram.

1.6 β^- Decay

In β^- decay, electrons (β^- particles) are emitted, converting a neutron into a proton in the nucleus:

$$ {}^{1}_{0}\mathrm{n} \longrightarrow {}^{1}_{1}\mathrm{p}^{+} + \mathrm{e}^{-} + \bar{\nu}_\mathrm{e}. \tag{12} $$

Thus, the atomic number Z increases by 1, and the neutron number N decreases by 1. The mass number A remains the same, transitioning the element to its successor in the periodic table. β^- decay typically affects nuclides with an excess of neutrons. Additionally, an electron antineutrino $\bar{\nu}_\mathrm{e}$ is created, preserving the lepton number. The general reaction for a β^- decay is

$$ {}^{\mathrm{A}}_{\mathrm{Z}}\mathrm{X} \longrightarrow {}^{\mathrm{A}}_{\mathrm{Z+1}}\mathrm{Y}^{+} + \mathrm{e}^{-} + \bar{\nu}_\mathrm{e} + Q. \tag{13} $$

Neglecting the (very small) mass of the neutrino, the Q-value is calculated from the mass balance

$$ Q = \left[m\left({}^{\mathrm{A}}_{\mathrm{Z}}\mathrm{X}\right) - m\left({}^{\mathrm{A}}_{\mathrm{Z+1}}\mathrm{Y}\right) \right] c^2. \tag{14} $$

Note that the daughter atom is initially singly positively ionized, as its proton number has increased by 1. This charge difference is compensated by capturing a free electron from its surroundings, becoming a neutral atom. This additional electron taken from the surroundings balances in mass with the electron produced in the β^- decay. Hence, the produced electron does not appear separately in the mass balance.

An example is the β^- decay of ^{60}Co (Fig. 2):

$$ {}^{60}_{27}\mathrm{Co} \longrightarrow {}^{60}_{28}\mathrm{Ni}^{+} + \mathrm{e}^{-} + \bar{\nu}_\mathrm{e} + 2.822\,\mathrm{MeV}. \tag{15} $$

1.7 β^+ Decay

In β^+ decay, positrons (β^+ particles) are emitted, converting a proton into a neutron in the nucleus:

$$ {}^{1}_{1}\mathrm{p}^{+} \longrightarrow {}^{1}_{0}\mathrm{n} + \mathrm{e}^{+} + \nu_\mathrm{e}. \tag{16} $$

β^+ decay typically affects nuclides with an excess of protons. The atomic number Z decreases by 1, and the neutron number increases by 1. The element transitions to its predecessor in the periodic table. Additionally, an electron neutrino ν_e is created, preserving the lepton number:

$$ {}^{\mathrm{A}}_{\mathrm{Z}}\mathrm{X} \longrightarrow {}^{\mathrm{A}}_{\mathrm{Z-1}}\mathrm{Y}^{-} + \mathrm{e}^{+} + \nu_\mathrm{e} + Q. \tag{17} $$

The mass balance of β^+ decay now has an additional term compared to (14):

$$ Q = \left[m\left({}^{\mathrm{A}}_{\mathrm{Z}}\mathrm{X}\right) - m\left({}^{\mathrm{A}}_{\mathrm{Z-1}}\mathrm{Y}\right) - 2m_\mathrm{e} \right] c^2. \tag{18} $$

The daughter atom is initially singly negatively ionized, as its proton number has decreased by 1. This is compensated by releasing an electron from the atomic shell into its surroundings. In the balance, it appears as if an electron has been created in the decay, along with the positron. Therefore, the mass balance includes the combined rest mass of the positron and the electron ($2m_\mathrm{e}c^2 = 2 \times 511\,\mathrm{keV}$). Thus, β^+ decay can only occur if at least a decay energy of 1022 keV is available.

An example is the β^+ decay of ^{22}Na (Fig. 3):

$$ {}^{22}_{11}\mathrm{Na} \longrightarrow {}^{22}_{10}\mathrm{Ne}^{-} + \mathrm{e}^{+} + \nu_\mathrm{e} + 1.821\,\mathrm{MeV}. \tag{19} $$

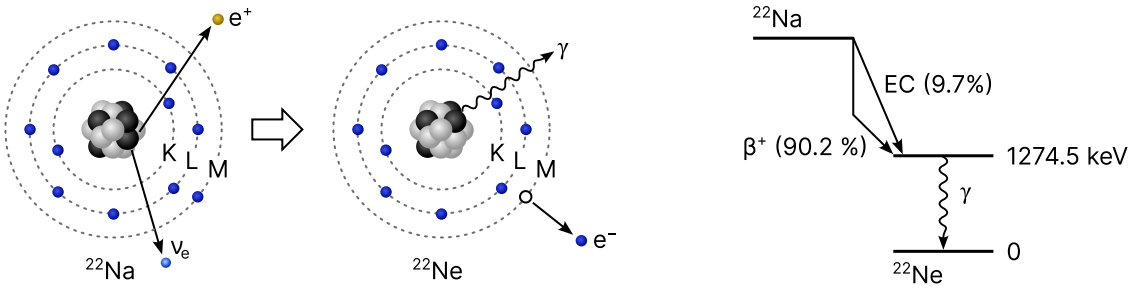

Figure 3: The β^+ decay of Sodium-22 (left). In the decay, a positron e^+ is produced, and the daughter atom ^{22}Ne additionally releases an electron into its surroundings to achieve a neutral state. In the energy level diagram (right), it is shown that for the β^+ process, an initial energy of 1022 keV is required, whereas this energy is not needed for the EC process (electron capture).

1.7.1 Positron Annihilation Radiation

The positron produced in the β^+ decay moves through the surrounding material and is decelerated by Coulomb interaction with the local electric fields of the atomic shells. Once it comes to rest, it quickly annihilates with an electron in its local environment. In the process, two photons are created, each with 511 keV, which, due to the conservation of momentum, move away from each other in opposite directions.

$$e^+ + e^- \longrightarrow \gamma + \gamma \tag{20}$$

The electron-positron system is not completely at rest with respect to the laboratory reference frame before annihilation. Due to the Doppler effect, the individual energies of the annihilation photons can deviate from 511 keV. However, their sum always amounts to exactly $2m_e c^2 = 1022$ keV. In typical laboratory setups, often only one of the two annihilation photons can be detected, as the second photon will move away from the detector surface due to the opposite directions, especially if the sample lies flat on the detector and is not enclosed by it. The resulting 511 keV peak often experiences a Doppler broadening due to the variable energy of the individual annihilation photons.

1.7.2 Electron Capture (EC) and X-ray Fluorescence

Instead of generating a positron, it can also occur that an electron from the atomic shell is captured to combine with a proton (Fig. 4, left). This is most likely for electrons close to the nucleus, as the wave functions overlap most strongly in this region. This process is called **electron capture (EC),** sometimes denoted with an ε.

$${}^1_1p^+ + e^- \longrightarrow {}^1_0n + \nu_e \tag{21}$$

The captured electron leaves a vacancy in the atomic shell, which is filled by a less tightly bound electron from a higher shell. This electron, in turn, leaves a vacancy at its original place in the energy space (Fig. 4, right). In this way, a multi-stage cascade of electron transitions can occur. The energy difference of these transitions is usually compensated by the emission of an **X-ray photon,** which is also detectable. Therefore, catalogs of known energies of gamma emitters typically also list the corresponding X-ray energies.

Instead of emitting an X-ray photon, the transition energy can also be transferred to another electron in the atomic shell. Normally, this completely breaks the electron's bond to the atom: the atom is ionized and an **Auger electron** is emitted.

Although in electron capture neither an electron nor a positron is created, it is still considered a form of beta decay.

In the case of ^{22}Na shown as an example above, electron capture can also occur as an alternative process to β^+ decay with a probability of about 10 % (Fig. 3, right, and Fig. 4):

$${}^{22}_{11}\mathrm{Na} \longrightarrow {}^{22}_{10}\mathrm{Ne} + \nu_e + 2.843\,\mathrm{MeV}. \tag{22}$$

Since no electron or positron is produced in this process, the Q-value here is 1022 keV higher (double the rest mass of an electron or positron) than in the β^+ decay of ^{22}Na (reaction 19).

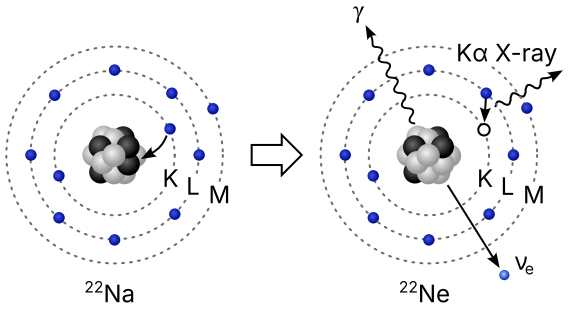

Figure 4: Electron capture (left) and subsequent X-ray fluorescence (right), when the vacancy created by the capture is filled by an electron from a higher shell.

1.8 Nuclide Charts

Nuclide charts provide a clear representation of nuclides and their properties. The most common is the Segrè representation, where the neutron number increases along the horizontal axis, and the proton number increases along the vertical axis (Fig. 5). Typically, the nuclides are displayed as points color-coded by their most probable decay type. One of the most well-known is the **Karlsruhe Nuclide Chart,** which includes additional information such as half-life and probabilities of different decay types.

From such a representation, it becomes quickly apparent that β^- decays dominate in nuclei with an excess of neutrons, and β^+ decays in nuclei with an excess of protons. Between these two groups lies a "valley of stable nuclides." α decays dominate in heavier nuclei, and in very heavy nuclei, spontaneous fission becomes more probable.

Nuclide charts make it very easy to determine the daughter nuclide of a decay:

- In **α decay,** a helium nucleus is emitted, i.e., two neutrons and two protons. N and Z each decrease by 2. The daughter nuclide is therefore located two steps diagonally to the lower left in the nuclide chart.
- In **β^- decay,** a neutron is converted into a proton. N decreases by 1, Z increases by 1. The daughter nuclide is therefore located one step diagonally to the upper left in the nuclide chart.
- In **β^+ decay,** a proton is converted into a neutron: N increases by 1, Z decreases by 1. The daughter nuclide is located one step diagonally to the lower right.

The β decay types thus move towards the "valley of stable nuclides."

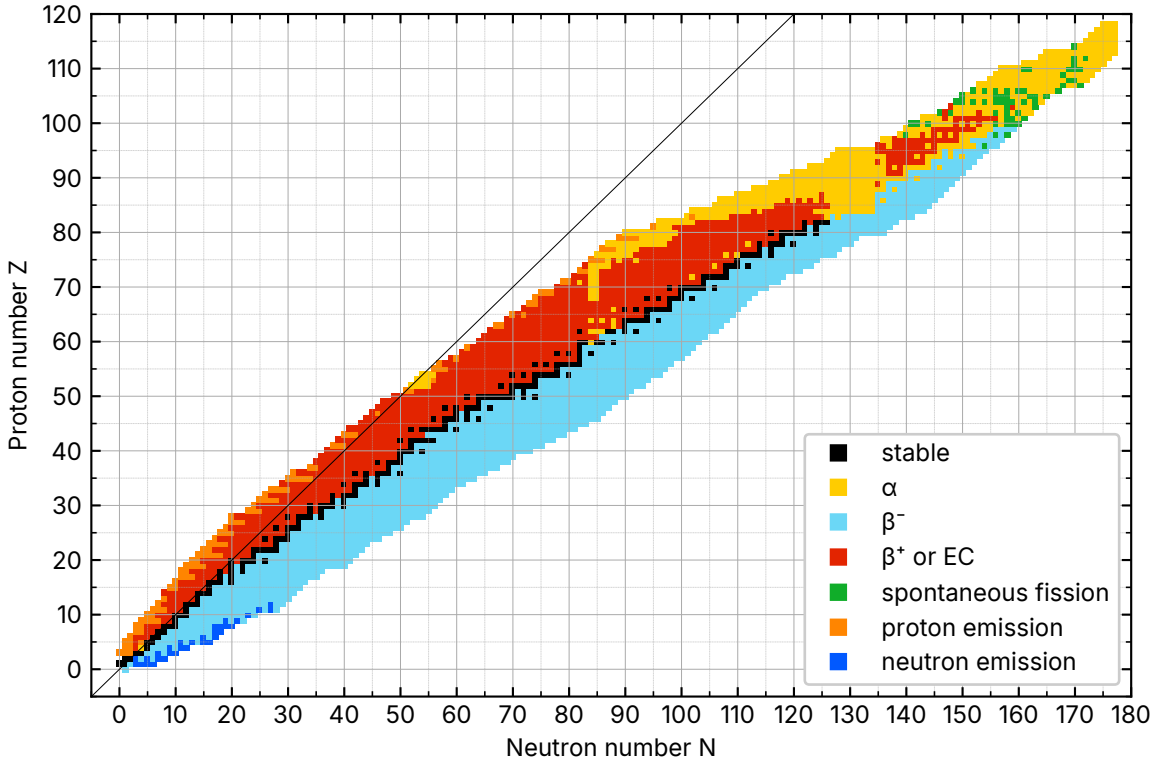

Figure 5: Simplified nuclide chart. The primary decay type of the nuclides is color-coded. Created from data in the Nubase2020 database. [1]

1.9 Decay Chains

After a radioactive decay, the daughter nuclide is not necessarily in a stable state, but can undergo a series of further decays until a stable nucleus is reached. The heavier naturally occurring radionuclides can each be assigned to one of four **natural decay chains.** These end in stable isotopes of lead or thallium.

While the mass number A decreases by 4 in alpha decay, it remains constant in beta decays. Thus, the mass number of all nuclei in a specific decay chain can be assigned as

$$A(n) = 4n + k. \tag{23}$$

Here, n is an integer; for the offset, the possibilities are $k = 0, 1, 2, 3$. For $k \geq 4$, repetitions occur, which could be compensated for by reducing n. The offset k thus identifies the specific natural decay chain in the nomenclature of nuclear physicists.[2] All four decay chains are listed by name in Table 1. They are shown in detail in Section 4.3 along with their respective half-lives and gamma energies.

The Neptunium series, except for ^{209}Bi, no longer occurs naturally on Earth and is only accessible through artificially produced radionuclides.

Table 1: Natural decay chains

A	Decay chain	
$4n$	Thorium series	^{232}Th
$4n+1$	Neptunium series	^{237}Np
$4n+2$	Uranium series	^{238}U
$4n+3$	Actinium series	^{235}U

1.10 Natural and Artificial Radionuclides

Naturally occurring radionuclides were either formed by stellar nucleosynthesis or are continually recreated on Earth through cosmic radiation[3], or are intermediate products of the natural decay chains.

Those radionuclides that were present at the formation of the Earth and have not yet completely decayed are referred to as **primordial radionuclides.** This includes the heavier elements that start the natural decay chains: ^{232}Th, ^{235}U, and ^{238}U. However, there are also about 30 other, sometimes lighter, primordial radionuclides. Using gamma spectrometry, the primordial ^{40}K ($t_{1/2} = 1.248 \times 10^9$ years) can be very well detected in the natural gamma background. It is incorporated into the human body through potassium-rich foods, contributing to our natural exposure to gamma radiation.

Artificial Radionuclides are produced during technically induced nuclear reactions, especially in reactors for energy production or during nuclear weapons tests. Radionuclides also enter the Earth's atmosphere as a result of reactor accidents like the Chernobyl nuclear disaster on April 26, 1986. From the atmosphere, it is deposited in the soil or accumulated by living beings. Especially ^{137}Cs is detectable in the gamma background, which is produced in the fission of ^{236}U during a nuclear reaction:

$$^{235}_{92}\mathrm{U} + {}^{1}_{0}\mathrm{n} \rightarrow {}^{236}_{92}\mathrm{U} \rightarrow {}^{137}_{55}\mathrm{Cs} + {}^{96}_{37}\mathrm{Rb} + 3\,{}^{1}_{0}\mathrm{n}. \tag{24}$$

An overview of the gamma energies of the background radiation is provided in Table 4 in Section 4.2.

1.11 Further Decay and Relaxation Mechanisms

1.11.1 Internal Conversion (IC)

The energy of an excited nucleus can also be transferred to an electron: this is then ejected from the atomic shell. Here, the nucleus does not relax into its ground state through the emission of γ-radiation, but X-rays and Auger electrons are produced. This process is called **internal conversion (IC)**.

1.11.2 Spontaneous Fission (SF)

Heavy nuclei can also decay into two relatively large nuclear fragments. This process is called **spontaneous fission (SF).** For the gamma spectrometry in this experiment, this process is not of importance.

1.11.3 Isomeric Transition (IT)

After a decay, the relaxation from the excited nuclear state into the ground state typically occurs extremely quickly through the emission of

gamma radiation. The daughter nuclei usually remain in their excited state for less than a picosecond. However, it may happen that the lifetime of the excited state extends over a much longer period. From a nanosecond upwards, this is called a **metastable state.** Although the excited nucleus does not differ in proton or neutron number from its ground state, it is considered an independent nuclide: it is then referred to as an **isomer.** In nuclide charts and decay chains, it is usually marked with a lower-case *m*. When the isomer finally relaxes into a more energetically favorable state, this is called an **isomeric transition (IT).** An example is the metastable state ^{234m}Pa within the Uranium series (Table 7) with a half-life of 1.17 min.

2 Interaction of Gamma Radiation with Matter

2.1 General

Gamma radiation is a form of ionizing radiation. The high-energy photons ionize the atoms of the matter they encounter. In semiconductors like the germanium detector used in this experiment, they generate entire cascades of electron-hole pairs. Only through this process is it possible to accurately determine the energy of the photons. Ionization occurs in different ways, which are briefly presented below.

2.2 Photoelectric Absorption

In the photoelectric effect (Fig. 6), the entire energy of a photon is transferred to an electron. With high-energy gamma radiation, this leads to the electron being ejected from its bond to the atomic nucleus, i.e., to the **ionization** of the atom. The electron leaves the atom with a kinetic energy E_{kin}, which is given by the energy E_γ of the photon, minus the binding energy E_b to the atomic nucleus:

$$E_{\mathrm{kin}} = E_\gamma - E_\mathrm{b}. \tag{25}$$

Tightly bound electrons close to the nucleus (K and L shell) are preferentially ejected from the atom, as long as the energy of the gamma photon is sufficient. Lower energy radiation, on the other hand, ionizes the more weakly bound electrons of higher shells.

The ejected, fast electrons in turn interact with other electrons in the vicinity, thereby gradually generating new electron-hole pairs in the semiconductor. A cascade effect occurs.

The ionized atom remains initially in an excited state with the energy E_b above its ground state. However, it soon relaxes to the ground state, either by redistributing the excitation energy among the remaining electrons (which can lead to further ionization) or by having higher-energy electrons fill the created vacancy. In the latter process, the energy difference is typically emitted in the form of **X-rays**. These X-ray photons are in turn absorbed by atoms in the vicinity, possibly causing another photoelectric effect, or they leave the detector and are thus lost. In the latter case, this leads to a measurement error: part of the energy of the gamma photon is *not* converted into electron-hole pairs that could be counted. This is a relatively rare event, which is especially likely when absorption occurs at the detector surface.

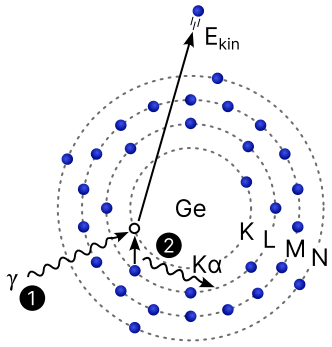

Figure 6: Photoelectric effect (1) and subsequent X-ray fluorescence (2): an L electron fills the remaining vacancy on the K shell.

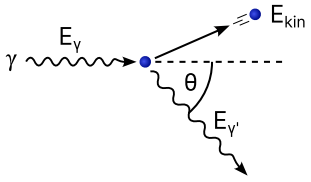

Figure 7: Compton scattering of a photon by an electron.

2.3 Compton Scattering

Compton scattering (Fig. 7) refers to the inelastic scattering of photons by electrons. Unlike the photoelectric effect, only a part of the photon's energy E_γ is transferred to the electron. The photon loses energy and changes its direction according to the conservation of momentum.

The kinetic energy of the electron E_{kin} and the scattering angle θ are related by

$$E_{\mathrm{kin}} = E_\gamma \left(1 - \frac{1}{1 + E_\gamma(1-\cos\theta)/m_e c^2}\right), \quad (26)$$

with the rest energy of the electron being $m_e c^2 = 511\,\mathrm{keV}$. This equation applies to Compton scattering on free electrons. In the case of bound electrons, their binding energy E_b must be subtracted. Since this is very small compared to the energy of a gamma photon, even atomically bound electrons can be considered as quasi-free in a first approximation. For the energy $E_{\gamma'}$ of the scattered photon, it follows that

$$E_{\gamma'} = E_\gamma - E_{\mathrm{kin}}. \quad (27)$$

From equation (26) two extreme cases are apparent: at complete forward scattering ($\theta = 0$) no energy is transferred to the electron. On the other hand, even at complete backscattering ($\theta = 180°$) only part of the photon's energy is transferred to the electron. The entire angular dependency of equation (26) is illustrated in Fig. 8 for an example photon energy of $E_\gamma = 500\,\mathrm{keV}$.

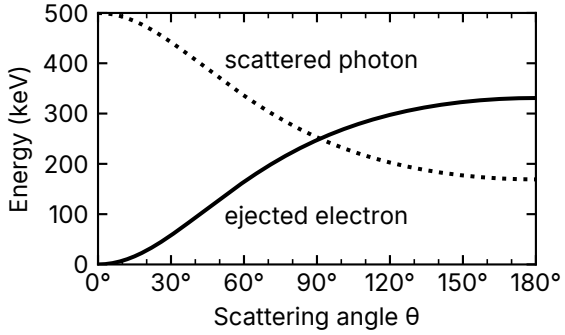

Figure 8: Energy of scattered particles in Compton effect as a function of the scattering angle θ for a photon energy of $E_\gamma = 500\,keV$.

2.4 Pair Production

A photon can be converted into an electron-positron pair in the Coulomb field of an atom. In this **pair production** (Fig. 9), the photon disappears completely. This process can only take place for photons which have an energy of at least the combined rest mass of the electron and positron, i.e., $2 \times 511\,\mathrm{keV} = 1022\,\mathrm{keV}$. If the photon's energy exceeds this threshold, the excess is converted into the kinetic energy of the electron and positron. Additionally, a very small portion is used for the recoil of the atom in whose Coulomb field the pair production occurs.

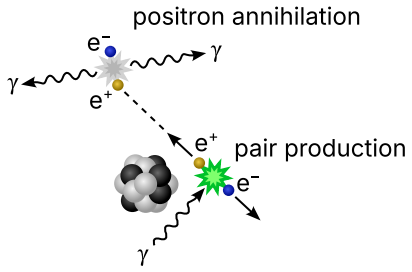

Figure 9: Formation of an electron-positron pair and subsequent annihilation of the positron with an electron in its vicinity.

As with the two previously discussed processes, the electron and positron interact with other atoms as they move through the surrounding material, ionizing them, which leads to the generation of additional free charge carriers. In this way, they lose their kinetic energy and eventually come to rest. The positron that has come to rest now annihilates extremely quickly with an electron in its local vicinity. Here, the combined rest energy (1022 keV) produces two gamma quanta, each with an energy of 511 keV, which move away from each other in opposite directions due to the conservation of momentum. Normally, the electron-positron system is not completely at rest relative to the laboratory reference system at the time of annihilation, as the positron may have some residual kinetic energy and electrons bound to atoms possess angular momentum. Therefore, a corresponding Doppler shift of the photon energies can be observed. In high-resolution gamma spectrometry, this leads to the peaks of positron annihilation radiation being a little bit broader than those of characteristic gamma radiation from excited atomic nuclei.

Very little time elapses between pair production and the annihilation of the positron, typically on the order of a nanosecond.

3 Experimental Fundamentals

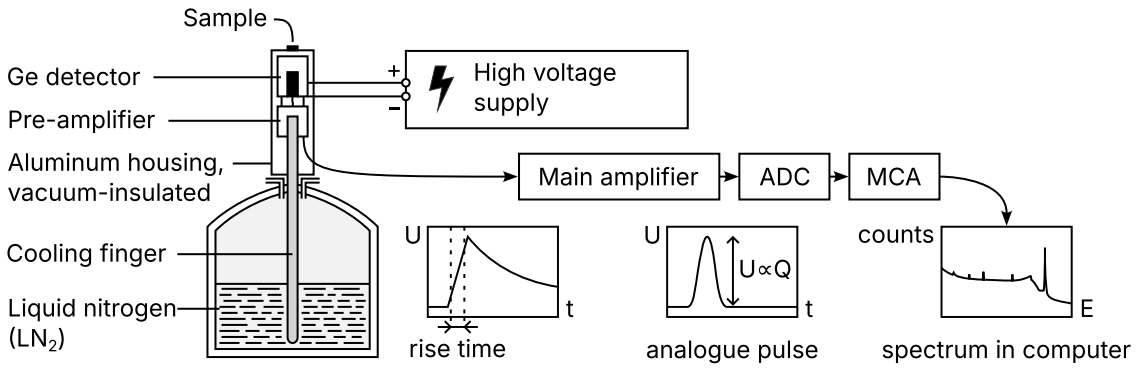

Figure 10: Setup of the gamma spectrometer and signals of the electronic processing stages.

3.1 General Experimental Setup

The heart of the gamma spectrometer (Fig. 10) is a semiconductor detector made of germanium. It is located in a vacuum chamber inside of an aluminum housing. It is cooled via a cooling finger that is immersed in a tank filled with liquid nitrogen.

Incoming gamma photons generate electron-hole pairs in the semiconductor detector, which are extracted via an applied electric field and later counted. This allows for the determination of the energy of the gamma quanta: the number of electron-hole pairs is proportional to the photon energy. The extracted charges are temporarily stored in a capacitor in the pre-amplifier.

The signal voltage at the pre-amplifier is transmitted via a cable to the main amplifier, where a sharp rise in voltage is transformed into an analog voltage pulse, the height of which is proportional to the detected energy of the gamma photon (i.e., the integrated rising edge from the pre-amplifier's capacitor). The peak height is converted into a digital number by the *analog-to-digital converter (ADC)* and passed to the *multi-channel analyzer (MCA)*, which creates a histogram from the individual digital signals, i.e., records the actual spectrum.

3.2 Semiconductor Detector

Semiconductor detectors operate on the principle of ionization: incoming photons or particle radiation ionize the material, i.e., they generate free charge carriers, which are extracted via an electric field and electronically counted. The number of generated free charge carriers is proportional to the energy of the photon. Unlike gas ionization or scintillation detectors, semiconductors offer great advantages: the ionization energy is in the range of a few electronvolts due to the small distance between the valence and conduction band. Moreover, solids offer a high particle density and thus a significantly higher absorption coefficient than, for example, a gas volume. For each incoming photon, a huge number of charge carriers can be lifted into the conduction band in a short time, resulting in a high energy resolution. Free charge carriers can be extracted from the detector and counted relatively quickly: this results in a short dead time, i.e., successive events can be reliably distinguished even at short intervals.

The detector volume should contain as few free charge carriers as possible to minimize leakage currents that arise from the external electric field. It is impractical to manufacture semiconductor crystals with the necessary purity. Therefore, a p-n junction (Fig. 11) is used, where foreign atoms are deliberately introduced into the semiconductor crystal. This process is called **doping.** Germanium is a tetravalent element: each germanium atom has four electrons on its outer shell and thus forms a covalent bond with four neighboring germanium atoms by creating delocalized electron pairs. This forms a tetrahedral crystal structure in space (diamond structure).

If a few tetravalent germanium atoms are replaced by trivalent atoms during doping (e.g., B, Al, Ga), electron vacancies (so-called *holes*) are created, which cannot participate in bonds. Such doping is called **p-doping:** the holes are effectively considered to be positive charge carriers.

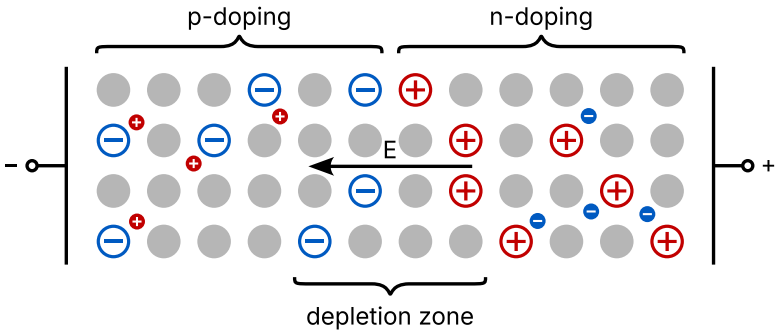

Figure 11: p-n junction in a Ge semiconductor detector. The lattice of germanium atoms (gray filled circles) is doped with foreign atoms: trivalent elements create freely movable holes in the case of p-doping, pentavalent elements create freely movable electrons in the case of n-doping. Along the interface of both regions, a depletion zone forms without free charge carriers. Due to the electric charges of the remaining ion nuclei, an electric field $\vec{E}$ forms, which counteracts the diffusion of free charge carriers. If an additional electric field were applied externally across the electrodes shown, the depletion zone would expand.

Conversely, doping the crystal with pentavalent elements (e.g., P, As, Sb) introduces an additional electron into the crystal that also does not participate in a bond. This type is called **n-doping**, since it introduces negative charge carriers into the crystal. Both the holes and the additional electrons are only weakly bound to the atomic nuclei of their host atoms. Even at room temperature, they are usually delocalized in the crystal, forming a hole or electron gas. Such doped crystals are electrically conductive, yet electrically neutral, since the doping is done with electrically neutral atoms.

Connecting a p-doped and an n-doped region results in a **p-n junction** (Fig. 11). Due to diffusion, free electrons and holes recombine at the interface between the two materials. The missing electrons and holes no longer compensate their corresponding countercharge in the doped atomic nuclei, leading to the formation of an electrically negative charge zone in the p-doped area and an electrically positive one in the n-doped area. An electric field is created that counteracts the diffusion of the free charge carriers from the outside. At a certain field strength, a balance is established between the repelling field and the charge carrier diffusion outside the field. A **depletion zone** (also called *space-charge layer*) forms at the interface, which contains no free charge carriers. Applying an external voltage enhances the electric field and the depletion zone grows, as the free charge carriers from the surrounding regions are drawn out. Therefore, a semiconductor detector is effectively a p-n diode operated in reverse bias.

The interaction probability of gamma photons with matter is rather low. Therefore, it is desirable to have a large detector volume with a big depletion zone to detect as many incoming photons as possible. The applied high voltage expands the depletion zone to the detector volume and ensures that the electron-hole pairs created by the gamma photons do not immediately recombine, but are separated and transported outward to the electrodes and into the counting device. In practice, it is not possible to build arbitrarily large detectors, as it is challenging to maintain very high voltages (breakdown voltage, electrical discharges, etc.). The extent of the detection volume is typically a few centimeters in all spatial directions.

At room temperature, germanium has a relatively small band gap of only 0.67 eV between the valence and conduction bands. As a consequence, valence electrons are lifted into the conduction band, thus providing a very high number of free charge carriers in the depletion zone: this intrinsic conductivity would lead to high leakage currents. For this reason, a germanium detector must be cooled with liquid nitrogen (maximum 77 K or −196 °C).

In a first approximation, one might assume that the number of free electrons n_e generated by an incoming photon with energy E is determined by the semiconductor's band gap ΔE_{gap} such that the photon's energy is split up into a multiple of the band gap: $n_e = E/\Delta E_{gap}$. In fact, the aver-

age energy required to generate an electron-hole pair is about a factor of 3 higher (Tab. 2). The reason is that electrons can be excited to higher states in the conduction band, from which they subsequently relax into the energetically lowest possible state in the conduction band by generating lattice vibrations (phonons). This process is called *thermalization.*

	Si	Ge
Band gap (eV)	1.107	0.67
e^-h^+ generation (eV)	3.62	2.96

Table 2: Material properties of Si and Ge: Band gap and average energy required to generate an electron-hole pair (e^-h^+).

3.3 Counting Electronics

When an incoming photon generates a certain amount of free charge carriers in the detector, these are transported by the detector voltage to the electrodes and collected in the capacitor of the **pre-amplifier** (Fig. 10). This leads to a rapid voltage rise at the pre-amplifier, which then discharges comparatively slowly. The time required to charge the capacitor in the pre-amplifier from 10 % to 90 % of the total charge generated by the incoming photon is called **rise time.** It characterizes how quickly a gamma event can be read out: the shorter the rise time, the faster two pulses can follow each other and still be resolved individually. The rise time is typically about 100 ... 500 ns. In comparison, the capacitor discharge time ("fall time") is about 50 to 150 µs. For further signal processing, however, only the steep edge of the voltage rise is relevant. This is integrated in the **main amplifier** to form an analog voltage pulse, the height U of which is proportional to the collected charge quantity Q (Fig. 10, bottom).

The voltage pulse from the main amplifier is then digitized in the **Analog-Digital Converter (ADC).** The analog voltage is converted into a digital number. The accuracy depends on how many bits are available to the ADC. For example, a 13-bit ADC can convert an analog voltage into a number between 0 and $2^{13} - 1 = 8191$. Accordingly, in this example, a total of 8192 bins, called **channels,** are available for accumulating the energy histogram. This leads to a certain minimal energy difference that can be resolved by the ADC: the channel width.

Each gamma event thus leads to a digital channel number issued by the ADC, which is proportional to the energy of the event. In the **Multi-Channel Analyzer (MCA),** all events are counted: it creates and stores a histogram of how often each channel number (energy) occurred. This is the actual gamma spectrum.

To assign the channels of the spectrum to an energy, i.e., to convert the horizontal axis of the histogram from channels to an energy unit (usually keV), a calibration with known reference sources must be carried out. The calibration standards available in the lab are listed in Table 3 in Section 4.1.

During the electronic processing of an event, the system is blocked from detecting any further events. This period, during which no new events can be detected, is called **dead time.**

3.4 Sample Placement

For soil samples and liquid samples, standardized **Marinelli beakers** have been established. They are designed to be airtight and to enclose the detector housing as much as possible to maximize the counting rate. Smaller samples, especially for calibration, are also placed in an empty Marinelli beaker on the detector housing during the experiment. This prevents an accidental loss of the samples. As the plastic material of the beakers hardly absorbs any gamma radiation, this measure has no negative effect on the measurement.

3.5 Features of Gamma Spectra

The interactions of gamma radiation with matter discussed in Section 2, in combination with a detector that is limited in size, lead to various features that typically appear in a gamma spectrum. These features are introduced in this section using the example spectrum of ^{28}Al, which is shown in Fig. 12.

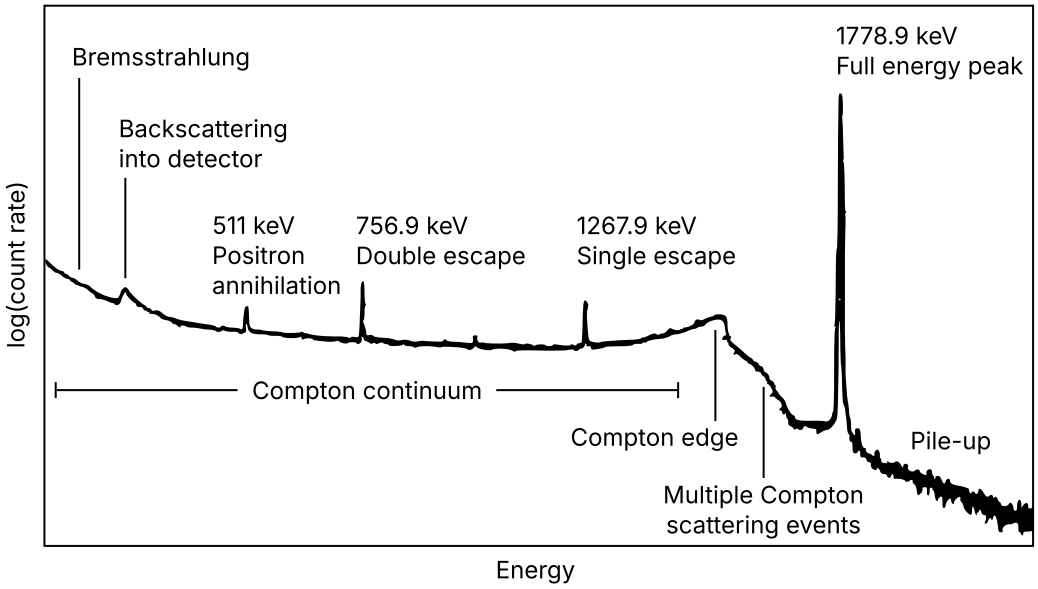

Figure 12: Example spectrum for ^{28}Al, with the typical features labeled. Taken from Gilmore.[4]

^{28}Al is a pure β^- emitter with a single gamma line at 1778.987 keV. When the complete energy of a photon is captured by the detector, the so-called **Full Energy Peak** is formed. This represents the actual energy of the gamma photons emitted by the source. Since the detector is not infinite in size, gamma photons can escape from the detector without transferring their entire energy to the semiconductor material. When photons generate free charge carriers from Compton scattering and subsequently escape from the detector, they contribute to the so-called **Compton continuum.** According to the Klein-Nishina formula, the cross-section for Compton scattering is angle-dependent, and scattering angles of $\theta = 0$ (forward scattering) and $\theta = 180°$ (backscattering) are more likely than angles in between. This leads to an accumulation at the **Compton edge** at the high-energy end of the Compton continuum. This represents the maximum energy transferable in Compton scattering. At the low-energy end of the Compton continuum, there is the **Compton backscatter peak,** caused by photons that are backscattered into the detector from the detector's housing. These backscattered photons have already transferred most of their energy to electrons outside of the detector (Fig. 8) and thus form a peak in the low-energy region of the Compton continuum.

Since the gamma energy of ^{28}Al exceeds 1022 keV, pair production can occur in the detector. During the annihilation of the positron, two annihilation photons, each with 511 keV, move away from each other in opposite directions (see Section 2.4). If one of the two annihilation photons leaves the detector and the rest of the energy is otherwise completely captured, this contributes to the **Single Escape Peak,** which lies 511 keV below the Full Energy Peak. If both annihilation photons leave the detector, this contributes to the **Double Escape Peak,** which accordingly has 1022 keV less energy than the Full Energy Peak.

Pair production does not necessarily have to take place in the detector itself but can also occur in the sample or in the detector housing. In this case, the detector might still capture one of the two annihilation photons; the other will move away from the detector in the opposite direction. This leads to the formation of the **Positron Annihilation Peak** at 511 keV. This is also typical for β^+ emitters, where positrons are created during the decay and annihilate directly in the sample. Above the Full Energy Peak, a shoulder of further, rather rare events can form: the so-called **pile-up** occurs when more than one photon is detected simultaneously. **Bremsstrahlung** is generated when fast charge carriers are decelerated in a material. This is a typical feature in the gamma spectra of β emitters, as their decay produces fast electrons or positrons. The Bremsstrahlung spectrum overlaps with the gamma spectrum in the low-energy range.

3.6 Line Width, Resolution, and Peak-to-Compton Ratio

The peaks in a gamma spectrum have a certain width that corresponds to an energy uncertainty (Fig. 13). A characteristic measure for the resolution of a spectral peak is its Full Width at Half Maximum (FWHM). According to the IEEE Standard 325-1996, the FWHM of the 1332.5 keV line of ^{60}Co is used to determine the energy resolution of a gamma spectrometer with a germanium semiconductor detector.

The **energy resolution** R is then defined as the resolvable line width as a fraction of the total energy $E_{\max}$ at the peak maximum:

$$R = \mathrm{FWHM}/E_{\max}. \tag{28}$$

Another important measure of the quality of a gamma spectrometer is the **Peak-to-Compton Ratio**. To calculate it, the maximum count rate in the 1332.5 keV peak of ^{60}Co is divided by the average count rate of the Compton continuum in the energy range $E = 1040 \ldots 1096$ keV.[5]

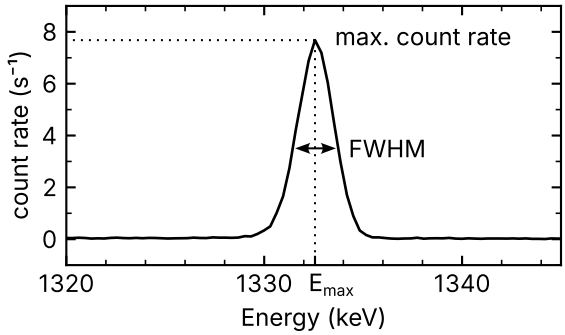

Figure 13: The 1332.5 keV peak of ^{60}Co shows a certain line width characterized by the FWHM.

3.7 Sources of Error

The energy uncertainty ΔE, which causes the line width, has four main sources,

$$\Delta E^2 = \Delta E_{\mathrm{i}}^2 + \Delta E_{\mathrm{e}}^2 + \Delta E_{\mathrm{c}}^2 + \Delta E_{\mathrm{p}}^2. \tag{29}$$

The **intrinsic uncertainty** ΔE_{i} already exists in the gamma energies emitted by the excited nuclei. According to the Heisenberg uncertainty principle, the energy uncertainty δE and the lifetime δt of an excited state are inversely proportional:

$$\delta E \cdot \delta t \geq \hbar/2\pi. \tag{30}$$

In the case of β^- decay of ^{60}Co, the excited 1332.5 keV state of the daughter nuclide has a half-life of about 0.9 ps, which corresponds to an intrinsic line width of 1.1×10^{-3} eV. This is very small compared to the other uncertainties and even to the usual channel width of a spectrometer and can usually be neglected.

The remaining three uncertainty contributions are of a statistical nature and are therefore referred to as **statistical uncertainties**.

The **electronic noise** ΔE_{e} of the readout electronics can be reduced by using high-quality components and by cooling.

During charge transport out of the detector, charges can be lost if, for example, they are captured by unoccupied recombination centers (defects) in the semiconductor crystal or by unsaturated chemical bonds at interfaces. This contributes to the **charge collection uncertainty** ΔE_{c}. In the detector's dead layer, it can also happen that generated electron-hole pairs are not separated, but immediately recombine.

Finally, there is the **production uncertainty** ΔE_{p} in the generation of free charge carriers. As described in Section 3.2 about the semiconductor detector, energy can be transferred into lattice vibrations and is therefore lost for detection. Photons of the same energy will thus generate different numbers of free charge carriers, even when their energy is completely deposited inside the detector.

The intrinsic uncertainty ΔE_{i} originates from a Lorentz distribution, while the other (statistical) fluctuations are Gaussian distributed. Strictly speaking, a gamma peak is the convolution of a Lorentz function and a Gaussian function,[1] a so-called Voigt profile. Since the intrinsic uncertainty is negligible and its distribution can be assumed as an almost ideal δ-peak, in practice it is often sufficient to fit a Gaussian distribution to the gamma peak being examined.

[1] The convolution of the Gaussian distributions of the three statistical uncertainties is, again, a (broader) Gaussian distribution.

4 Lists of Known Gamma and X-ray Energies

4.1 Calibration Standards for Gamma Radiation Detectors

For the calibration of gamma spectrometers, calibration standards with known emission energies are used. The X-ray and gamma energies of the nuclides used in this experiment are listed in Table 3. They are based on the *XGAMMA* catalog[6] of the IAEA and are taken from: *Gilmore: Practical Gamma-ray Spectrometry.*[7]

For emitted X-rays, the respective designation of the daughter atom's X-ray line is provided. Otherwise, it is either gamma radiation (γ) from the nucleus of the daughter nuclide or positron annihilation radiation (511 keV). Additionally, the emission probability P_γ is given.

Table 3: Gamma and X-ray standards for detector calibration.[7]

Nuclide	Decay	$t_{1/2}$ (years)	Origin	Energy (keV)	P_γ (%)
^{22}Na	ε	2.602	annihilation	511.0	179.8(2)
			γ	1274.537(3)	99.94(14)
^{60}Co	β^-	5.27	γ	1173.228(3)	99.85(3)
			γ	1332.492(4)	99.9826(6)
^{133}Ba	ε	10.551	Cs Kα_2	30.625	34.0(4)
			Cs Kα_1	30.973	62.8(7)
			Cs Kβ_1	30.09(17)	18.2(2)
			Cs Kβ_2	35.89(7)	4.6(1)
			γ	53.1622(6)	2.14(3)
			γ	79.6142(12)	2.65(5)
			γ_a	80.9979(11)	32.9(3)
			γ	160.6120(16)	0.638(5)
			γ	223.2368(13)	0.453(3)
			γ	276.3989(12)	7.16(5)
			γ	302.8508(5)	18.34(13)
			γ_b	356.0129(7)	62.05(19)
			γ	383.8484(12)	8.94(6)
			$\gamma_a + \gamma_b$	437.0108	
^{137}Cs	β^-	30.08	Ba Kα_2	31.8174	1.95(4)
			Ba Kα_1	32.1939	3.59(7)
			Ba Kβ_1	36.49(18)	1.055(22)
			Ba Kβ_2	37.34(9)	0.266(8)
			γ	661.657(3)	84.99(20)
^{241}Am	α	432.6	Np L1	11.89(2)	0.848(10)
			Np Lα	13.9(2)	13.03(10)
			Np Lβη	17.81(2)	18.86(15)
			Np Lγ	20.82(2)	4.81(4)
			γ	26.3446(2)	2.4(3)
			γ	33.1963(3)	0.121(3)
			γ	59.5409(1)	35.78(9)

4.2 Gamma and X-Ray Energies in Background Radiation

Table 4: Gamma and X-Ray Energies in Background Radiation.[8]

Energy (keV)	Parent nuclide	P_γ (%)	Origin
8.04	Cu Kα	29.3	Fluorescence from shielding
8.91	Cu Kβ	4.7	Fluorescence from shielding
22.98	Cd $K\alpha_2$	24.5	Fluorescence from shielding
23.17	Cd $K\alpha_1$	46.1	Fluorescence from shielding
25.04	Sn $K\alpha_2$	24.7	Fluorescence from shielding
25.27	Sn $K\alpha_1$	45.7	Fluorescence from shielding
26.10	Cd $K\beta_1$	7.69	Fluorescence from shielding
26.64	Cd $K\beta_2$	1.98	Fluorescence from shielding
28.49	Sn $K\beta_1$	7.99	Fluorescence from shielding
29.11	Sn $K\beta_2$	2.19	Fluorescence from shielding
46.54	**^{210}Pb**	4.25	^{238}U (^{226}Ra) series
53.23	^{214}Pb	1.06	^{238}U (^{226}Ra) series
53.44	^{73m}Ge	10.34	^{72}Ge(n, γ), ^{72}Ge(n, 2n)
63.28	**^{234}Th**	4.8	^{238}U series
67.70	^{230}Th	0.38	^{238}U series
68.75	^{73*}Ge		^{72}Ge(n, n′) broad asymmetric peak
72.81	Pb $K\alpha_2$	27.7	Fluorescence and ^{208}Tl decay
74.82	**Bi $K\alpha_2$**	27.7	$^{212,\,214}$Pb decay
74.97	Pb $K\alpha_1$	46.2	Fluorescence and ^{208}Tl decay
77.11	**Bi $K\alpha_1$**	46.2	$^{212,\,214}$Pb decay
79.29	Po $K\alpha_1$	46.1	Fluorescence and $^{212,\,214}$Bi decay
81.23	^{231}Th	0.9	^{235}U series
84.94	Pb $K\beta_1$	10.7	Fluorescence and ^{208}Tl decay
87.30	Pb $K\beta_2$	3.91	Fluorescence and ^{208}Tl decay
87.35	Bi $K\beta_1$	10.7	$^{212,\,214}$Pb decay
89.78	Bi $K\beta_2$	3.93	$^{212,\,214}$Pb decay
89.96	Th $K\alpha_2$	28.1	^{235}U and ^{228}Ac decay
92.58	**^{234}Th**	5.58	^{238}U series (doublet)
93.35	Th $K\alpha_1$	45.4	^{235}U and ^{228}Ac decay
99.60	^{228}Ac	1.37	^{232}Th series
105.60	Th $K\beta_1$	10.7	^{235}U and ^{228}Ac decay
109.16	^{235}U	1.54	Primordial
112.81	^{234}Th	0.28	^{238}U series
113.10	^{227}Th	0.74	^{235}U series
122.32	^{223}Ra	1.192	^{235}U series
129.06	^{228}Ac	2.42	^{232}Th series
131.20	^{234}Pa	20	^{238}U series
139.68	^{75m}Ge	39	^{74}Ge(n, γ), ^{76}Ge(n, 2n) isomeric transition
143.76	^{235}U	10.96	Primordial
154.20	^{223}Ra	5.59	^{235}U series
159.70	^{77m}Ge	10.33	^{76}Ge(n, γ) isomeric transition
163.33	^{235}U	5.08	Primordial
174.95	^{71m}Ge		^{70}Ge(n, γ) activation
185.72	**^{235}U**	57.2	Primordial
186.21	**^{226}Ra**	3.555	^{238}U series

Table 4: Gamma and X-Ray Energies in Background Radiation[8] *(continued)*.

Energy (keV)	Parent nuclide	P_γ (%)	Origin
198.39	^{71m}Ge		^{70}Ge(n, γ) sum: 23.5 +174.95 keV
205.31	^{235}U	5.01	Primordial
209.26	^{228}Ac	3.89	^{232}Th series
215.50	^{77m}Ge	21	
216.00	^{228}Th	0.3	^{232}Th series
226.80	^{234}Pa	11.4	^{238}U series
236.00	^{227}Th	11.65	^{235}U series
238.63	**^{212}Pb**	43.6	^{232}Th series
240.89	^{224}Ra	4.12	^{232}Th series
242.00	^{214}Pb	7.268	^{238}U (^{226}Ra) series
256.00	^{227}Th	7.6	^{235}U series
269.49	^{223}Ra	13.7	^{235}U series
270.24	^{228}Ac	3.46	^{232}Th series
271.20	^{219}Rn	9.9	^{235}U series
277.37	^{208}Tl	2.37	^{232}Th series
278.26	^{64*}Cu		^{63}Cu(n, γ), ^{65}Cu(n, 2n) prompt γ
295.22	**^{214}Pb**	18.5	^{238}U (^{226}Ra) series
299.98	^{227}Th	2.16	^{235}U series
300.07	^{231}Pa	2.47	^{235}U series
300.09	^{212}Pb	3.18	^{232}Th series
302.70	^{231}Pa	2.24	^{235}U series
323.30	^{223}Ra	3.9	^{235}U series
328.00	^{228}Ac	2.95	^{232}Th series
330.10	^{231}Pa	1.31	^{235}U series
336.24	^{115m}Cd / ^{115m}In	45.9	Cd activation (daughter of ^{115}Cd)
338.28	^{223}Ra	2.79	^{235}U series
338.32	^{228}Ac	11.27	^{232}Th series
351.06	^{211}Bi	12.91	^{235}U series
351.93	**^{214}Pb**	35.6	^{238}U (^{226}Ra) series
401.70	^{219}Rn	6.64	^{235}U series
404.80	^{211}Pb	3.83	^{235}U series
409.46	^{228}Ac	1.92	^{232}Th series
416.86	^{116m}In	27.7	^{115}In(n, γ) activation
427.00	^{211}Pb	1.72	^{235}U series
444.90	^{223}Ra	1.27	^{235}U series
447.60	^{7}Be	10.44	Cosmic
452.83	^{212}Bi	0.36	^{232}Th series
462.00	^{214}Pb	0.213	^{238}U (^{226}Ra) series
463.00	^{228}Ac	4.4	^{232}Th series
510.70	^{208}Tl	6.29	^{232}Th series
511.00	**annihilation**		β^+ and Doppler broadening
527.90	^{115}Cd	27.5	^{114}Cd(n, γ) activation
549.70	^{220}Rn	0.1	^{232}Th series
558.46	^{114*}Cd		^{113}Cd(n, γ) prompt γ
569.70	^{207m}Pb	97.87	^{207}Pb(n, n′)
570.82	^{228}Ac	0.182	^{232}Th series
579.20	^{207*}Pb		^{207}Pb(n, n′) prompt γ
583.19	**^{208}Tl**	30.6	^{232}Th series

Table 4: Gamma and X-Ray Energies in Background Radiation[8] *(continued)*.

Energy (keV)	Parent nuclide	P_γ (%)	Origin
595.85	^{74*}Ge		^{74}Ge(n, n′) broad asymmetric peak
609.31	**^{214}Bi**	45.49	^{238}U (^{226}Ra) series
661.66	^{137}Cs	84.99	Fission
669.62	^{63*}Cu		^{63}Cu(n, n′) prompt γ
689.60	^{72*}Ge		^{72}Ge(n, n′) broad asymmetric peak
726.86	^{228}Ac	0.62	^{232}Th series
727.33	^{212}Bi	6.74	^{232}Th series
755.31	^{228}Ac	1.0	^{232}Th series
768.36	^{214}Bi	4.891	^{238}U (^{226}Ra) series
794.95	^{228}Ac	4.25	^{232}Th series
803.06	^{206*}Pb		^{206}Pb(n, n′) prompt γ
806.17	^{214}Bi	1.262	^{238}U (^{226}Ra) series
832.01	^{211}Pb	3.52	^{235}U series
835.71	^{228}Ac	1.61	^{232}Th series
839.04	^{214}Pb	0.587	^{238}U (^{226}Ra) series
843.76	^{27}Mg	71.8	^{26}Mg(n, γ) or ^{27}Al(n, p) of encapsulation
846.77	^{56*}Fe		^{56}Fe(n, n′)
860.56	^{208}Tl	4.48	^{232}Th series
911.20	**^{228}Ac**	25.8	^{232}Th series
934.06	^{214}Bi	3.096	^{238}U (^{226}Ra) series
962.06	^{63*}Cu		^{63}Cu(n, n′)
964.77	^{228}Ac	4.99	^{232}Th series
968.97	**^{228}Ac**	15.8	^{232}Th series
1001.03	^{234m}Pa	1.021	^{238}U series
1014.44	^{27}Mg	28	^{26}Mg(n, γ) or ^{27}Al(n, p) of encapsulation
1063.66	^{207m}Pb	88.5	^{207}Pb(n, n′)
1097.30	^{116}In	56.2	^{115}In(n, γ) activation
1115.56	^{65*}Cu		^{65}Cu(n, n′)
1120.29	^{214}Bi	14.907	^{238}U (^{226}Ra) series
1155.19	^{214}Bi	1.635	^{238}U (^{226}Ra) series
1173.23	^{60}Co	99.85	Activation
1238.11	^{214}Bi	5.827	^{238}U (^{226}Ra) series
1293.54	^{116}In	84.4	^{115}In(n, γ) activation
1332.49	^{60}Co	99.98	Activation
1377.67	^{214}Bi	3.967	^{238}U (^{226}Ra) series
1407.98	^{214}Bi	2.389	^{238}U (^{226}Ra) series
1459.14	^{228}Ac	0.83	^{232}Th series
1460.82	**^{40}K**	10.66	Primordial
1588.20	^{228}Ac	3.22	^{232}Th series
1620.74	^{212}Bi	1.51	^{232}Th series
1630.63	^{228}Ac	1.51	^{232}Th series
1729.60	^{214}Bi	2.843	^{238}U (^{226}Ra) series
1764.49	**^{214}Bi**	15.28	^{238}U (^{226}Ra) series
1847.42	^{214}Bi	2.023	^{238}U (^{226}Ra) series
2204.21	^{214}Bi	4.913	^{238}U (^{226}Ra) series
2224.57	^{2*}H		^{1}H(n, γ)
2614.51	**^{208}Tl**	35.85	^{232}Th series, ^{208}Pb(n, p)

4.3 Natural Decay Chains

The following tables list the four natural decay chains and give the most common gamma lines along with their respective probabilities P_γ.

Table 5: Thorium Series (^{232}Th)

Nuclide	Half life	γ Energies (keV)	P_γ (%)
^{232}Th	1.41×10^{10} a		
α			
^{228}Ra	5.75 a		
β^-			
^{228}Ac	6.15 h	99.6	1.37
		129.1	2.45
		209.3	3.88
		270.2	3.43
		328.0	2.95
		338.3	11.25
		409.5	1.94
		463.0	4.44
β^-		772.4	1.58
		794.9	4.34
		835.7	1.68
		911.2	26.60
		964.8	5.11
		969.0	16.17
		1588.2	3.27
		1630.6	1.60
^{228}Th	1.910 a	84.37	1.6
α		216.0	0.3
^{224}Ra	3.64 d	241.0	3.97
α			
^{220}Rn	55 s	549.7	0.1
α			
^{216}Po	0.15 s		
α			
^{212}Pb	10.64 h	238.6	43.6
β^-		300.1	3.34
^{212}Bi	60.6 min	39.86	1.10
		288.1	0.34
		452.98	0.36
		727.3	6.65
		785.4	1.11
		1620.6	1.51
β^- (64 %) / α (36 %)			
^{212}Po	304 ns		
α			
^{208}Tl	3.05 min	277.4	6.31
		510.8	22.60
		583.2	84.50
		860.6	12.42
β^-		2614.5	99.20
^{208}Pb	stable		

Table 6: Actinium Series (^{235}U)

Nuclide	Half life	γ Energies (keV)	P_γ (%)
^{235}U	7.04×10^8 a	143.8	10.9
		163.3	5.00
α		185.7	57.50
		205.3	5.00
^{231}Th	25.5 h	81.5	1.29
β^-		84.2	6.60
^{231}Pa	3.276×10^4 a	27.4	9.3
		283.7	1.60
α		300.0	2.39
		302.7	2.24
		330.1	1.31
^{227}Ac	21.6 a		
β^- (98.6 %) α (1.4 %)			
^{227}Th	18.718 d	49.9	0.52
		50.1	7.28
α		236.0	11.65
		256.0	7.6
^{223}Fr	22 min	50.8	34.0
		80.0	8.16
β^-		234.6	3.4
^{223}Ra	11.43 d	122.3	1.19
		144.2	3.26
		154.2	5.59
α		269.4	13.6
		323.9	3.9
		338.3	2.78
		444.9	1.27
^{219}Rn	4.0 s	271.2	9.9
α		401.7	6.64
^{215}Po	1.78 ms		
α ($\approx$ 100 %) β^- (0.000 23 %)			
^{211}Pb	36.1 min	404.8	3.83
		427.0	1.72
β^-		831.8	3.8
^{215}At	0.1 ms		
α			
^{211}Bi	2.14 min	351.0	12.76
β^- (0.28 %) α (99.7 %)			
^{211}Po	0.52 s	569.65	0.53
		897.8	0.52
α			
^{207}Tl	4.79 min	897.77	0.24
β^-			
^{207}Pb	stable		

Table 7: Uranium Series (^{238}U)

Nuclide	Half life	γ Energies (keV)	P_γ (%)
^{238}U	4.51×10^9 a		
α			
^{234}Th	24.1 d	63.3	4.49
β^-		92.6	5.16
^{234}Pa^m	1.17 min	766.42	0.317
β^- (99.87 %) / IT (0.13 %)		1001.03	0.842
^{234}Pa	6.75 h	131.2	20.0
		226.8	11.4
		569.3	13.5
		882.0	28.0
		926.4	24.9
β^-		946.0	12.0
^{234}U	2.47×10^5 a	53.2	0.12
α			
^{230}Th	8.0×10^4 a	67.7	0.38
α		143.9	0.05
^{226}Ra	1602 a	186.1	3.5
α			
^{222}Rn	3.823 d		
α			
^{218}Po	3.05 min		
α (99.98 %) / β^- (0.02 %)			
^{214}Pb	26.8 min	241.9	7.46
		295.2	19.20
β^-		351.9	37.10
^{218}At	2 s		
α			
^{214}Bi	19.9 min	609.3	46.10
		768.4	4.88
		934.0	3.16
		1120.3	15.00
		1155.2	1.63
		1238.1	5.92
		1377.6	4.02
		1408.0	2.48
		1729.6	3.05
		1764.5	15.90
β^- (99.98 %) / α (0.02 %)		2204.1	4.99
^{214}Po	163.6 µs	799.7	0.01
α			
^{210}Tl	1.3 min	296.0	79.16
		795.0	98.95
		1060.0	12.37
		1210.0	16.82
β^-		1310.0	20.78
^{210}Pb	22.3 a	46.5	4.05
β^-			
^{210}Bi	5.01 d		
β^-			
^{210}Po	138.4 d	803.0	0.0011
α			
^{206}Pb	stable		

Table 8: Neptunium Series (^{237}Np)

Nuclide	Half life	γ Energies (keV)	P_γ (%)
^{241}Am	432.6 a	26.345	2.27
		33.196	0.126
α		59.541	35.9
^{237}Np	2.14×10^6 a	29.374	14.5
		86.484	12.2
α		92.282	1.43
		95.863	2.3
^{233}Pa	26.974 d	94.654	8.9
		98.434	14.2
β^-		300.128	6.54
		311.901	38.2
		340.477	4.44
^{233}U	159.2×10^3 a	42.435	0.072
		42.633	0.0132
α		54.704	0.0168
		97.135	0.0203
^{229}Th	7340 a	85.431	14.7
		88.471	23.9
α		99.432	2.93
		100.13	5.61
		193.52	4.41
		210.853	2.8
^{225}Ra	14.9 d	12.7	13.6
β^-		40.09	30.0
^{225}Ac	10.0 d	83.231	0.75
		86.105	1.23
α		99.8	1.0
		150.1	0.6
^{221}Fr	4.801 min	218.0	11.44
		81.517	1.47
α		78.948	0.89
^{217}At	32.6 ms	257.89	0.0287
		335.26	0.0062
α		593.13	0.0115
^{213}Bi	45.59 min	292.8	0.419
		440.45	25.9
		807.36	0.289
α (2.14 %)	β^- (97.86 %)	1100.17	0.252
^{209}Tl	2.162 min	117.21	76.0
		465.14	95.4
β^-		1567.08	99.663
^{213}Po	3.72 μs	778.87	0.0044
α			
^{209}Pb	3.234 h		
β^-			
^{209}Bi	1.9×10^{19} a		
α			
^{205}Tl	stable		

References

[1] F.G. Kondev, M. Wang, W.J. Huang, S. Naimi, and G. Audi. The NUBASE2020 evaluation of nuclear physics properties. *Chinese Physics C*, 45(3):030001, March 2021. doi:10.1088/1674-1137/abddae. URL https://www-nds.iaea.org/amdc/.

[2] Theo Mayer-Kuckuk. Zerfall instabiler Kerne. In *Kernphysik*, page 74. Teubner, 7th edition, 2002. ISBN 3-519-13223-0.

[3] Winfried Koelzer. *Lexikon zur Kernenergie. Ausgabe Januar 2019*. KIT Scientific Publishing, 2019. doi:10.5445/KSP/1000088491. URL https://publikationen.bibliothek.kit.edu/1000088491.

[4] Gordon Gilmore. Interaction of gamma radiation with matter. In *Practical Gamma-Ray Spectrometry*, page 33. John Wiley & Sons, Ltd, 2nd edition, 2008. ISBN 9780470861981. doi:10.1002/9780470861981.ch2.

[5] D. Arnold, K. Debertin, A. Heckel, G. Kanisch, H. Wershofen, and C. Wilhelm. Grundlagen der Gammaspektrometrie (γ-SPEKT/GRUNDL in: Messanleitungen für die Überwachung radioaktiver Stoffe in der Umwelt und externer Strahlung). *Bundesministerium für Umwelt, Naturschutz, nukleare Sicherheit und Verbraucherschutz*, March 2018. ISSN 1865-8725. URL https://www.bmuv.de/fileadmin/Daten_BMU/Download_PDF/Strahlenschutz/strlsch_messungen_gamma_grund_bf.pdf.

[6] X-ray and Gamma-ray Decay Data Standards for Detector Calibration and Other Applications. Technical report, International Atomic Energy Agency (IAEA), December 2005. URL https://www-nds.iaea.org/xgamma_standards/.

[7] Gordon Gilmore. Appendix B: Gamma- and X-Ray Standards for Detector Calibration. In *Practical Gamma-Ray Spectrometry*, pages 351–357. John Wiley & Sons, Ltd, 2nd edition, 2008. ISBN 9780470861981. doi:10.1002/9780470861981.app2.

[8] Gordon Gilmore. Appendix D: Gamma-Ray Energies in the Detector Background and the Environment. In *Practical Gamma-Ray Spectrometry*, pages 361–364. John Wiley & Sons, Ltd, 2nd edition, 2008. ISBN 9780470861981. doi:10.1002/9780470861981.app4.